NATIONAL ADVISORY COMMITTEE FOR AERONAUTICS

TECHNICAL NOTE 2418

FLOW SEPARATION AHEAD OF BLUNT BODIES AT SUPERSONIC SPEEDS

By W. E. Moeckel

Lewis Flight Propulsion Laboratory
Cleveland, Ohio

Washington
July 1951

NATIONAL ADVISORY COMMITTEE FOR AERONAUTICS

TECHNICAL NOTE 2418

FLOW SEPARATION AHEAD OF BLUNT BODIES AT SUPERSONIC SPEEDS

By W. E. Moeckel

SUMMARY

Supersonic flow against blunt bodies placed in boundary layers or wakes is discussed qualitatively, and it is concluded that wedge-shaped or conical dead-air regions should form ahead of the body if part of the upstream velocity profile is subsonic and if the body is fairly thick relative to the initial boundary layer or wake thickness. Quantitative analysis of this type of flow indicates, however, that for each free-stream Mach number, there is also a maximum relative body thickness beyond which wedge-type or conical-type separation regions cannot occur. This maximum relative body thickness is large for high Mach numbers but approaches zero for a Mach number of 1.

For the intermediate range of body thicknesses, an analysis of the two-dimensional flow against blunt bodies mounted on a flat plate agreed quantitatively with experimental results in the Mach number range of 1.73 to 2.02. As the body thickness approached the maximum theoretically possible for wedge-type separation, unsteady flow was observed. For bodies of the same order of thickness as the initial boundary layer, experimental pressures near the leading edge of the bodies remained higher than those predicted for wedge-type separation.

INTRODUCTION

When a blunt body is placed in a uniform supersonic stream, a detached shock wave forms ahead of it. This detached shock is normal in front of the body and decays gradually into a Mach wave at large distances from the body. If, however, the blunt body is placed in a region of nearly constant static pressure, but nonuniform stagnation pressure, such as a boundary layer or a wake, it becomes impossible to satisfy certain flow requirements unless the form of the shock is altered. Consider, for example, the sketch in figure 1(a) of a blunt body in a completely supersonic wake. If the static pressure ahead of the shock is assumed to be constant and the velocity gradient to be as indicated, the pressure behind a normal shock at the stagnation streamline would be less than the pressure behind the shock in the free stream.

With the dashed shock form shown, there would consequently be a positive pressure gradient toward the center line and a convergent flow behind the shock, which is an impossible situation. In any real flow, the pressure gradient normal to the stagnation streamline on the axis of symmetry must be zero or negative. Since the Mach number at the axis is lower than in the free stream, no shock will produce pressures at the axis as high as those behind the shock outside the shear layer as long as the stagnation point remains on the body. The required high pressure near the vertex of the shock can be attained only if the stagnation point moves upstream; hence a dead-air region will form (fig. 1(a)) which effectively changes the nose of the body to a form compatible with the flow requirements.

When the velocity near the axis is subsonic, as in a boundary layer, the high pressures in the dead-air region can feed upstream and modify the flow outside the boundary layer or wake until some sort of equilibrium is established. If the body is fairly thick relative to the shear layer, the dead-air region can become large relative to the thickness of the shear region. If the circulatory motions in this region are negligible, the boundary of the dead-air region must be a constant-pressure surface. Hence, the form of the dead-air region outside the boundary layer or wake should be that of a wedge for two-dimensional flow and a cone for axially symmetric flow (fig. 1(b)).

As the body thickness is increased indefinitely, it seems reasonable that a configuration different from that shown in figure 1(b) will occur. When the shear layer becomes insignificantly thin relative to the body, the detached-shock configuration encountered in uniform supersonic streams should reappear.

The purpose of the present paper is to investigate the nature of the equilibrium that determines the size of a wedge-type or cone-type separation region and the limits beyond which this type of separation cannot exist. For two-dimensional flow against blunt bodies mounted on a flat plate, theoretical predictions are compared with experimental results. This investigation was conducted at the NACA Lewis laboratory.

ANALYSIS

The initial analysis will be concerned with the flow against two-dimensional bodies mounted on a flat plate. The symbols used are defined in appendix A.

The analysis is based on the simplified picture of the separation phenomenon shown in figure 2. The curvature of the shock resulting from boundary-layer - shock-wave interaction is neglected, and the shock is assumed to remain straight and of constant intensity from the edge of the boundary layer to the point where the line perpendicular to the

dead-air boundary from the corner of the body intersects the shock. The dead-air region is assumed bounded by a straight line inclined at the angle λ to the flat plate and to have a constant pressure p_1 equal to the pressure behind the oblique shock. These assumptions should be approximately valid if the initial boundary-layer thickness δ_0 is small compared with the obstacle thickness b and if the circulatory motions in the dead-air region are negligibly small.

The continuity equation for the configuration in figure 2 is

$$\rho_0 u_0 (y_0 - \delta_0) + \int_0^{\delta_0} \rho u \, dy = \rho_1 u_1 (y_1 - \delta_1) + \int_0^{\delta_1} \rho u \, ds$$

which can be converted to

$$\rho_0 u_0 (y_0 - \delta_0^*) = \rho_1 u_1 (y_1 - \delta_1^*) \tag{1}$$

Since there is no friction force along the dead-air region, the momentum equation reads:

$$(p_1 - p_0) y_0 + \rho_1 u_1^2 \cos\lambda \, (y_1 - \delta_1) - \rho_0 u_0^2 (y_0 - \delta_0) + \int_0^{\delta_1} \rho u^2 \cos\lambda \, ds - \int_0^{\delta_0} \rho u^2 dy = 0$$

which, when combined with equation (1), can be converted to

$$y_0 \left(1 - \frac{u_1}{u_0} \cos\lambda - \frac{p_1 - p_0}{\rho_0 u_0^2} \right) = \theta_0 - \frac{\rho_1 u_1^2 \cos\lambda}{\rho_0 u_0^2} \theta_1 + \left(1 - \frac{u_1}{u_0} \cos\lambda \right) \delta_0^* \tag{2}$$

where θ_0 and θ_1 are the momentum thicknesses ahead of and at the end of the dead-air region, respectively. From oblique shock relations,

$$1 - \frac{u_1}{u_0} \cos\lambda = \frac{p_1 - p_0}{\rho_0 u_0^2} = \frac{1}{2} P_1$$

so that equation (2) becomes

$$\frac{\theta_1}{\theta_0} = \frac{1 + \frac{1}{2} h_0 P_1}{Q} \tag{3}$$

where

$$Q = \frac{\rho_1 u_1^2 \cos\lambda}{\rho_0 u_0^2} = \frac{p_1}{p_0} \frac{M_1^2}{M_0^2} \cos \lambda$$

and

$$h_0 = \frac{\delta_0^*}{\theta_0}$$

The parameters P_1, φ, and λ are related by the equation

$$\tan\lambda = \frac{\frac{1}{2} P_1 \cot\varphi}{1 - \frac{1}{2} P_1}$$

Hence equation (3) determines the equilibrium values of shock angle, detachment angle, or pressure in the dead-air region if θ_1/θ_0 is known. Precise determination of θ_1 depends on a knowledge of the profile between the dead-air region and the outer stream in the region downstream of the shock wave. Since this knowledge is not presently available, it will be of interest to see if a valid hypothesis concerning the magnitude of θ_1/θ_0 can be made.

The sketch of figure 2 suggests that a good estimation of θ_1 might be obtained by assuming that the increase of θ between station 0 and 1 due to mixing is proportional to the increase that would be expected if a solid wedge with angle λ replaced the dead-air region. With this assumption, the value of θ_1 becomes

$$\theta_1 = \theta_0 + \int_l^L \frac{\epsilon \tau_1}{\rho_1 u_1^2} \frac{dx}{\cos\lambda}$$

where ϵ is a factor of proportionaltiy.

When an average shear stress is used for the wedge, this equation becomes

$$\theta_1 - \theta_0 = \frac{\epsilon \tau_{1,av}}{\rho_1 u_1^2} \frac{b}{\sin \lambda} \tag{4}$$

With the assumption that the average shear stress on the replacing wedge differs little from the shear stress on the flat plate immediately ahead of the wedge, equation (4) becomes

$$\theta_1 - \theta_0 = \frac{\rho_0 u_0^2}{\rho_1 u_1^2} \epsilon \theta_0' \frac{b}{\sin \lambda}$$

because

$$\frac{\tau_0}{\rho_0 u_0^2} = \left(\frac{d\theta}{dx}\right)_{x = l} = \theta_0'$$

Rearrangement of the terms yields

$$\frac{\theta_1}{\theta_0} = 1 + \frac{\rho_0 u_0^2}{\rho_1 u_1^2} \frac{\epsilon \theta_0'}{\theta_0} \frac{b}{\sin \lambda} \tag{5}$$

Equating the values of θ_1/θ_0 from equations (3) and (5) yields

$$1 + \frac{\rho_0 u_0^2}{\rho_1 u_1^2} \frac{\epsilon \theta_0'}{\theta_0} \frac{b}{\sin \lambda} = \frac{1 + \frac{1}{2} h_0 P_1}{\frac{\rho_1 u_1^2}{\rho_0 u_0^2} \cos \lambda}$$

or

$$\epsilon \frac{\theta_0'}{\theta_0} b = \left(1 + \frac{1}{2} h_0 P_1 - Q\right) \tan \lambda = T \tan \lambda \tag{6}$$

Now, both for turbulent and for laminar flows along flat plates, formulas exist for the skin friction in the form

$$\theta' = \frac{\tau}{\rho_0 u_0^2} = k(M_0)\, R_x^{-1/\eta} \tag{7}$$

where η is 2 for laminar flow and approximately 7 for turbulent flow. Integration of equation (7) yields

$$\theta_0 = \int_0^l \theta'\, dx = \frac{\eta}{\eta-1}\, l\, k(M_0)\, R_l^{-1/\eta}$$

Hence,

$$\frac{\theta_0'}{\theta_0} = \frac{\eta-1}{\eta l} \tag{8}$$

and is independent of Mach number and Reynolds number to the extent that η is independent of these parameters.

Equation (6) now becomes

$$\epsilon \frac{b}{l} = \frac{\eta}{\eta-1}\, T \tan \lambda \tag{9}$$

or

$$\frac{b}{L} = \frac{T \tan \lambda}{\epsilon\left(\frac{\eta-1}{\eta}\right) + T} \tag{10}$$

since

$$l = L - b \operatorname{ctn} \lambda$$

When ϵ is specified, equation (10) gives the theoretical variation of φ, λ, or P_1 as a function of the thickness of the obstacle if the boundary layer ahead of the separated region is either completely turbulent or completely laminar. It appears reasonable that, for laminar boundary layer, the effective shear over the wedge should nevertheless be assumed equal to that of a turbulent boundary layer, inasmuch as the mixing region is probably turbulent regardless of the

state of the initial boundary layer. This modification is discussed in appendix B, where it is shown that the variation of b/L with λ can be calculated quite simply for this case from the values obtained for purely laminar flow. Modifications required when the boundary layer is partly laminar and partly turbulent are discussed in appendix C.

For turbulent boundary layers, values of h_0 required in equation (10) have been calculated as a function of M_0 in reference 1 for various power profiles of the form $\frac{u}{u_0} = \left(\frac{y}{\delta}\right)^{1/N}$. For laminar boundary layers, h_0 can be obtained from the profiles derived in reference 2. For the case of zero temperature gradient and a Prandtl number of 0.72 the equations of reference 2 yield

$$h = \frac{1.73 + 1.11(\gamma-1)M^2}{0.664} \tag{11}$$

Values of h as a function of M, obtained from reference 1 for $N = 7$ and from equation (11) are plotted in figure 3. With these values, the variation of λ and φ with b/L for turbulent and laminar boundary layers was computed for several Mach numbers for $\epsilon = 1.0$. The results are plotted in figure 4.[1] It will be noticed from this figure (particularly from fig. 4(b)) that, for each value of M_0, a maximum value of b/L is obtained beyond which the present analysis yields no solution. This maximum value occurs when the boundary-layer separation angle reaches the maximum flow-deflection angle for an attached oblique shock wave. For Mach numbers close to 1, wedge-type separation appears to be possible only for small values of b/L. For such small values of b/L, however, the effects of the boundary-layer shock-wave interaction become important. Hence, the present analysis is probably of interest primarily for high Mach numbers, where wedge-type separation is possible for fairly large values of b/L.

For values of b/L greater than the maximum value possible for wedge-type separation, it was expected that one of two possible configurations might occur: (1) A configuration similar to figure 1(a) might form ahead of the obstacle; or (2) the separation wedge might

---

[1]The effect of using other values of ϵ, as can be seen from equation (10), would be to shift the curves of figure 4 toward larger values of b/L for $\epsilon < 1$ and to smaller values of b/L for $\epsilon > 1$. No estimate of the magnitude of ϵ can yet be made from theoretical considerations, although it appears likely that the momentum change along a free surface should be less than along a solid surface. However, details of the shock - boundary-layer interaction may invalidate this expectation.

extend to the leading edge of the plate. Actually, as will be shown later, neither of these configurations was observed. Instead, the flow became unsteady even before the maximum analytical value of b/L was reached.

For large values of M_0, the present analysis yields negative values of b/L for weak shock waves. These negative values probably indicate again that details of the shock - boundary-layer interaction cannot be neglected when b is of the order of the thickness of the boundary layer. It will be noticed from equation (4) that the values of φ or λ obtained at $b = 0$ are those which would result if θ_1 were assumed equal to θ_0. With such an assumption there would be no variation of separation angle with body thickness, and separation angles other than zero would be obtained only at high Mach numbers.

APPARATUS AND PROCEDURE

A preliminary experiment to check analytical results was conducted in the NACA Lewis 18- by 18-inch tunnel, wherein a series of bars of rectangular cross section were mounted on a flat plate with a span of 16 inches. The angle of attack of the flat plate was variable such that a range of free-stream Mach numbers from 1.735 to 2.03 was obtainable. The Reynolds number per foot at a Mach number of 1.9 was 3.24×10^6.

For most tests, transition of the boundary layer was artificially induced by placing a 1/4-inch strip of carborundum dust across the plate, 3/4-inch from the leading edge. This strip was removed for some of the tests to check the effect of changing the initial velocity profile.

The flat-faced rods were mounted with their leading edges $8\frac{1}{2}$ inches from the leading edge of the plate. For values of b up to 3/4 inch, the rods extended over the full span of the plate. For thicker rods, however, choking of the tunnel occurred with full-span rods. Some of these rods were therefore reduced in length to obtain data for the larger values of b/L. The $1\frac{1}{4}$-inch thick rod, which was the thickest for which steady flow was obtained, had to be reduced to a span of 6 inches to avoid choking the tunnel. The effect of such reduction in span is shown in figure 5 for $b = 0.5$ inch. If it is assumed that the extent to which the flow is two-dimensional depends chiefly on the span-thickness ratio of the body, the results plotted in figure 5 indicate that for $1\frac{1}{4}$-inch rod (span-thickness ratio = 4.8) the boundary-layer detachment angle was reduced about $1\frac{1}{2}^\circ$ below that which would have been obtained for a more nearly two-dimensional body.

The variation of θ_0 with l along the flat plate with artificial transition was obtained at Mach number 1.88 in a previous investigation and is shown in figure 6(a). For comparison, a curve represented by the empirical formula

$$\theta_0 = \frac{7}{6} k(M_0) l R_l^{-1/7}$$

is also shown where $k(M_0)$ was taken equal to 0.0104. This value of $k(M_0)$ was obtained from the equations of reference 1 for a Mach number of 1.88. The empirical curve is somewhat higher than the experimental values probably because transition was induced artificially 3/4 inch from the leading edge. The boundary-layer thickness, according to reference 1, is about 12 times the momentum thickness at a Mach number of 1.9. In figure 6(b), values of θ_0'/θ_0 obtained from the experimental data and from equation (8) are plotted. The good agreement indicates that little error in the variation of b/L with separation angle should result from the use of empirical friction formulas. No boundary-layer surveys were made with natural transition on the plate.

COMPARISON OF THEORY AND EXPERIMENT

Schlieren photographs of the flow past the rectangular rods are shown in figure 7. The waves arising from the transition strip (which can be seen in most of the photographs) did not affect the determination of the Mach number upstream of the separation wedges since this Mach number was calculated using the static pressure measured by an orifice located 1/2-inch downstream of the transition strip. Another weak wave, about two-thirds of the distance from the leading edge of the plate to the model, resulted from a joint in the plate. As nearly as could be measured, this wave was inclined at the Mach angle; its effect on the flow was therefore considered negligible.

For small values of b/L, a steady flow pattern was obtained (figs. 7(a) to 7(c)). For values of b greater than $1\frac{1}{4}$ inches, however, unsteady flow of the type shown in figure 7(d) was obtained. For such flows the shock angle could not be measured, but a mean shock angle could be calculated from the pressure measurements in the separated region. For the steady configurations, the upstream edge of the waves that originate near the point of separation is curved in the vicinity of the boundary layer but becomes straight farther away from the plate. The initial curved portion results from boundary-layer interaction at the root of the shock wave, which was ignored in the analysis. In analyzing the data, the angle of the straight portion of the shock wave

was measured and compared with the shock angle calculated from the pressure in the dead-air region. The accuracy of the measured shock angle was low, however, because of the thickness of the trace; hence, the values of φ calculated from the pressure measurements were used for comparison of experiment with theory.

Turbulent Boundary Layer

The analytical and experimental variations of φ with b/L are compared in figure 8(a). The value of ϵ was taken equal to 1 for the analytical curves. Shown in figure 8(a) are all points obtained with the transition strip in place and with the models located $8\frac{1}{2}$-inches from the leading edge of the plate. The experimental points shown in figure 8(a) are not directly comparable with the theoretical curves because of the effect of reduced span-thickness ratio at large values of b/L. In order to provide more nearly comparable data, all values of φ obtained with span-thickness ratios less than 52 were corrected by an increment equal to the difference given in figure 5 between the value obtained at the actual span-thickness ratio and the value obtained for a span-thickness ratio of 32. These corrected values of φ are compared with the theoretical values in figure 8(b). The quantitative agreement between the experimental and the theoretical values of φ is quite good for values of b/L between 0.050 and 0.125.

Unsteady flow appeared for values of b/L greater than 0.15, which is considerably below the maximum values predicted by theory. This unsteadiness may result from the fact that two configurations are possible for large b; a modified bow wave could form or the separation could extend to the leading edge of the plate. The effective shock angles, computed from the measured mean pressure in the dead-air space, seem to increase rapidly just before the flow becomes oscillatory, as if a detached bow wave were forming, and then to drop to values that are lower than some of those obtained with steady flow. The shock angles that would be expected if the flow were separating at the leading edge of the plate ($\lambda = \tan^{-1} b/L$) are shown for comparison and the mean pressures appear to be of the order of magnitude corresponding to such separation. However, no definite conclusions can be drawn from these data since the nature of the unsteadiness of the flow is unknown, and hence the nature of the mean pressure cannot be established.

For values of b/L less than 0.075 (b/δ less than about 6), experimental values of φ remain higher than the theoretical values although they, too, should be equal to the Mach angle for $b/L = 0$.[2]

[2]The small angle due to the rate of increase of displacement thickness along the plate should be continuous for $b = 0$ and consequently should result in no finite disturbances.

The discrepancy between theory and experiment for low values of b/L is believed to result from the fact that the effect of the region of interaction of the boundary layer with the shock wave, which was neglected in the theory, becomes important as b approaches the thickness of the boundary layer (compare figs. 7(a) and 7(c)). The fact that experimental values remain higher than theoretical values for small b/L may indicate that the rate of change of momentum thickness in the region of shock - boundary-layer interaction is greater than along a solid surface.

Effect of Changes in Shear Profile

Shown in figure 9 are the values of φ obtained at $M_0 = 1.84$ when the models were moved to $5\frac{1}{2}$ inches from the leading edge with the transition strip still in place and the values of φ obtained for $L = 8\frac{1}{2}$ inches with the transition strip removed. These values are compared with various theoretical curves and with the experimental points from figure 8 for $L = 8\frac{1}{2}$ inches with artificial transition. The span-thickness ratios are shown for each data point to provide a valid basis for comparison of the effects of changes in the initial boundary layer.

Contrary to expectations, removal of the transition strip increased the strength of the shock for each value of b/L. This strength increase may indicate that separation originated in a region of transition rather than in the laminar region.[3] In such transition regions, θ_0' is considerably greater than in either laminar or turbulent regions, so that the average shear stress over the dead-air region should be higher, and consequently the shock should be stronger, than for completely laminar or turbulent flow. When the 1/2-inch model was placed $5\frac{1}{4}$ inches from the leading edge, on the other hand, the values of φ for comparable span-thickness ratios are lower than for $L = 8\frac{1}{2}$ inches. For $L = 5\frac{1}{4}$ inches, the separation region started only about 3 inches from the leading edge of the plate, so that the 3/4-inch region of laminar flow ahead of the transition strip could have a more pronounced influence on the separation angle than for $L = 8\frac{1}{2}$ inches. The theoretical curve for transition 3/4-inch from the leading edge, which was calculated from the equations in appendix C, agrees very well with the

---

[3] It seems probable that the separation itself introduces premature transition in the upstream laminar layer, so that separation angles corresponding to laminar flow ahead of the separation point may be observed experimentally only for quite low Reynolds numbers.

experimental point obtained with the largest span-thickness ratio. This point, as indicated in figure 5, is probably close to the true two-dimensional value. Theoretical curves resulting from the assumption of laminar flow on the plate and turbulent shear on the replacement wedge (appendix B) were calculated for comparison and indicate that, at the Reynolds number of the present tests, the nature of the boundary layer ahead of the separation is more significant than the magnitude of the assumed rate of increase of momentum thickness along the dead-air boundary. In view of the doubt whether separation of the type considered herein can occur without inducing transition ahead of the separation, these curves are probably only of academic interest.

DISCUSSION AND EXTENSION

Flow Patterns for Various Body-Thickness Ratios

On the basis of the experimental or analytical results presented in previous sections, it appears that the flow patterns obtained for a blunt body mounted on a flat plate with a supersonic free stream can be divided roughly into four types. These types are illustrated in figure 10 for a Mach number of approximately 1.9.

Type 1 (fig. 10(a)). - When the body is of the same order of thickness as the initial boundary layer, the shock - boundary-layer interaction is of primary importance and the analysis of the present paper is inapplicable. Data near a Mach number of 1.8 indicate that the body should be greater than about 5 times the boundary-layer thickness before agreement with the analysis is to be expected.

Type 2 (fig. 10(b)). - For a certain range of body thicknesses, the magnitude of which depends greatly on the free-stream Mach number, details of the shock - boundary-layer interaction become unimportant, and the analysis of this paper is applicable. The assumption that $\epsilon = 1$ appears to yield satisfactory agreement with experimental results in this flow region for the Mach number range investigated. For low supersonic Mach numbers, this type of flow may not appear at all.

Type 3 (fig. 10(c)). - As the body thickness approaches the maximum value for which the pattern of type 2 can exist, the flow becomes unsteady and the shock pattern appears to oscillate between a modified bow wave and the straight shock corresponding to separation from the leading edge of the plate. The sketch of figure 10(c) shows how the mean pressure in the dead-air region can become less than that corresponding to separation from the leading edge in this unsteady-flow region.

Type 4 (fig. 10(d)). - As the body thickness is increased further, the angle corresponding to separation at the leading edge approaches the maximum for which an attached shock is possible and a configuration

similar to that shown in figure 10(d) should appear. Except for the projection due to the presence of the plate, the shock location in this region should be calculable by the method of reference 3. If the plate does not extend beyond the foremost point of the detached shock corresponding to uniform flow, as calculated approximately by the method of reference 3, the presence of the plate should have negligible effect on the shock form, and the conventional bow wave, normal at the foremost point, should reappear. Whether the intermediate stage shown in figure 10(d) is stable remains to be established.

Axially Symmetric Flows

Discussion. - An extension of the method, whose completion awaits more knowledge of shear profiles, is the computation of the effective increases in fineness ratio and decreases in drag that can be realized by providing an initial boundary layer or wake ahead of a blunt-nosed axially symmetric body. Such a boundary layer or wake can be provided by extending a thin rod ahead of the nose (fig. 11) or by suspending a small body upstream of the nose to provide a wake. An effective conical nose of small weight can in this manner be provided for a blunt body, in the event that such a body is desirable for better utilization of space.

The use of dead-air regions to reduce the drag of blunt bodies has been suggested before, but no analysis was available to serve as a guide in the selection of a method for producing this dead-air region. The method shown in figure 11 seems the simplest and is amenable to analysis when the required friction data become available.

For this configuration, the cone angle and consequently the pressure drag can theoretically be reduced to as small a value as desired by increasing the thickness of the boundary layer or wake relative to the nose size. If the trend of the data for two-dimensional bodies occurs also for axially symmetric bodies, however, the rods required may become excesively long before pressure coefficients approaching zero can be realized (see fig. 8). Furthermore, as the ratio of the boundary layer or wake thickness to the nose radius increases, there is expected to be an increase in friction drag almost corresponding to that which would be obtained by replacing the projecting rod with separation cone by a solid cone. The optimum fineness ratio for the blunt body plus separation cone should therefore be almost the same as the optimum fineness ratio for a pointed-nose body. Although the length of rod required to yield a given fineness ratio cannot as yet be evaluated theoretically, the following analysis provides an indication of the chief parameters needed to solve the problem in the range of body thicknesses for which the flow is steady and the boundary layer is not too thick relative to the body.

Analysis. - By an analysis for axially symmetric flow similar to that used to obtain equation (3) for two-dimensional flow, the equation for the case shown in figure 12 is found to be

$$\frac{\theta_1^2}{\theta_0^2} = \frac{1 + h_0^2\left(1 - \frac{u_c}{u_0}\cos\lambda_c\right)}{Q_c} \tag{12}$$

where

$$Q_c = \frac{\rho_c u_c^2}{\rho_0 u_0^2}\cos\lambda_c$$

$$\theta_0^2 = 2\pi\int_a^{a+\delta_0} \frac{\rho u}{\rho_0 u_0}\left(1 - \frac{u}{u_0}\right) y\,dy$$

$$\theta_1^2 = 2\pi\int_b^{b+\delta_1\cos\lambda_c} \frac{\rho u}{\rho_c u_c}\left(1 - \frac{u}{u_c}\right)\frac{y\,dy}{\cos\lambda_c}$$

$$\delta_0^{*2} = 2\pi\int_a^{a+\delta_0} \left(1 - \frac{\rho u}{\rho_0 u_0}\right) y\,dy$$

$$\delta_1^{*2} = 2\pi\int_b^{b+\delta_1\cos\lambda_c} \left(1 - \frac{\rho u}{\rho_0 u_0}\right)\frac{y\,dy}{\cos\lambda_c}$$

and where subscript c refers to surface values corresponding to the separation cone half angle λ_c.

On the assumption that θ_1 and θ_0 are related approximately as they would be if a solid cone replaced the separation cone, another equation for θ_1^2/θ_0^2 can be derived and equated to the value of equation (12) to determine the cone separation angle.

If τ_c is the average shear force per unit area on the cone that replaces the dead-air region,

$$\frac{\theta_1^2}{\theta_0^2} = 1 + \frac{\tau_c}{\rho_c u_c^2}\frac{A_c}{\theta_0^2} \tag{13}$$

where A_c is the surface area of the cone and is given by

$$A_c = \pi b^2/\sin \lambda_c$$

if $\frac{a}{b} \ll 1$. From equations (12) and (13),

$$\left[1 + h_0^2\left(1 - \frac{u_c}{u_0}\cos\lambda_c\right) - Q_c\right]\tan\lambda_c \equiv T_c \tan\lambda_c = \frac{\tau_c}{\rho_0 u_0^2}\frac{\pi b^2}{\theta_0^2} \tag{14}$$

If the boundary-layer thickness on the projecting rod remains thin relative to the rod diameter, then the two-dimensional skin-friction formulas should be adequate for calculating θ_0^2. Thus, for $\delta_0 \ll a$,

$$\theta_0^2 \approx 2\pi a\int_0^{\delta_0}\frac{\rho u}{\rho_0 u_0}\left(1 - \frac{u}{u_0}\right)dy = 2\pi a\int_0^{l} k(M_0)R_x^{-1/\eta}\,dx$$

or

$$\theta_0^2 \approx 2\pi a l\,\frac{\eta}{\eta-1}\,k(M_0)R_l^{-1/\eta}$$

Now let β be the ratio of τ_c to the shear force per unit area on a flat plate τ_p and assume, as in the two-dimensional case, that τ_p is approximately equal to the shear stress at $x = l$. Then

$$\tau_c = \beta\tau_p = \beta\rho_0 u_0^2\,k(M_0)R_l^{-1/\eta}$$

and equation (14) becomes

$$T_c \tan\lambda_c = \frac{\eta-1}{\eta}\frac{\beta}{2}\frac{b}{a}\frac{b}{l} \tag{15}$$

Because

$$l = L - b \operatorname{ctn} \lambda_c$$

equation (15) can be written as

$$\frac{b}{L} = \frac{\frac{2}{\beta}\frac{a}{b} T_c \tan \lambda_c}{\frac{\eta}{\eta-1} + \frac{2}{\beta}\frac{a}{b} T_c} \tag{16}$$

The value of h_0^2 in T_c becomes approximately the two-dimensional form factor for $\delta_0 \ll a$ since

$$h_0^2 \approx \frac{2\pi a \int_0^{\delta_0} \left(1 - \frac{\rho u}{\rho_0 u_0}\right) dy}{2\pi a \int_0^{\delta_0} \frac{\rho u}{\rho_0 u_0}\left(1 - \frac{u}{u_0}\right) dy} = \frac{\delta_0^*}{\theta_0} = h_0$$

For a given ratio of rod radius to nose radius a/b, equation (16) expresses the variation of b/L with cone angle and Mach number when the boundary layer on the rod is entirely laminar or turbulent. Unfortunately, the magnitude of β is as yet unknown except for the case of laminar flow without initial boundary layer. It therefore seems advisable to postpone further discussion of equation (16) until a theoretical or experimental basis for estimating β becomes available.

Effect of Nose Shape

Most of the preceding discussions have assumed that the body has a flat nose or at least a sharp corner where the dead-air region terminates. For this type of body (wedge or cone) it is to be expected that the angle of the nose would have little effect on the shape of the dead-air region as long as the wedge or cone angle of the body is considerably greater than the wedge or cone angle of the dead-air region. Evidence to substantiate this expectation is given in reference 4, where wedges with half-angles from 14° to 90° were placed on the floor of a tunnel operating at a Mach number of 2.4. It is concluded in reference 4 that the foremost shock angle is approximately independent of wedge angle and that consequently the separation angle should be chiefly a function of Mach number and Reynolds number.

For bodies with curved noses, the point of contact of the dead-air boundary with the body should be the point where the slope of the body is equal to the slope of the dead-air boundary (see fig. 11). For the particular case of a circular nose,

$$b = r \cos \lambda \tag{17}$$

so that, for the two-dimensional case, equation (10) becomes

$$\frac{r}{L} = \frac{\frac{T \tan \lambda}{\cos \lambda}}{\frac{\eta-1}{\eta} + T} \tag{18}$$

which determines the separation angle as a function of the radius of the nose. If the nose is noncircular and if the equation of the nose contour is

$$y = f(x)$$

then b is the value of y for which $y' = \tan \lambda$.

Supersonic Diffusion by Means of Boundary-Layer Separation

Because the dead-air region ahead of blunt bodies tends to form a wedge or a cone for a range of values of b/L, it is feasible to form a supersonic inlet by placing a cowling around a configuration such as that shown in figure 11. Such an inlet should yield pressure recoveries that differ little from those obtained with inlets using solid cones or wedges as long as the mass flow into the inlet is the maximum possible. When the mass flow is reduced, this type of inlet may have lower additive drag due to spillage than the solid-body inlet, because the dead-air region will not support the pressure gradient across a strong detached shock wave. Consequently, the size and angle of the dead-air region should change as the mass flow is reduced. It remains to be demonstrated whether the separation inlet can be stable under reduced mass flow conditions.

CONCLUDING REMARKS

An analysis of supersonic flow against blunt bodies located in boundary layers or wakes indicates that wedge-type or conical-type dead-air regions occur only over a limited range of body thicknesses relative to the initial boundary layer or wake thickness. For the particular case

of two-dimensional blunt bodies mounted on a flat plate, quantitative agreement between predicted and experimental wedge-separation angles was obtained in this range of body thicknesses when the change in momentum thickness along the dead-air region was assumed to be equal to that which would be obtained if a solid wedge replaced the dead-air region. When the body thickness approached the maximum for which wedge-type separation was possible, unsteady flow was observed. For body thicknesses of the same order as the initial boundary layer thickness, shock angles larger than those predicted were obtained. This discrepancy was attributed to neglect of boundary-layer - shock-wave interaction in the analysis.

For low supersonic Mach numbers, the two-dimensional analysis indicated that the simple wedge-shaped dead-air region can exist only for body thicknesses that are of the same order of thickness as the initial boundary layer. For such bodies, however, details of the shock - boundary-layer interaction, which were neglected in the analysis, became important. The analysis given herein should therefore be of interest chiefly at high Mach numbers, where the cone or wedge-type separation can exist for bodies that are relatively thick compared with the initial boundary layer.

The unsteady flow observed when the body thickness approached the maximum possible thickness for wedge-type separation may result because two types of configuration are possible. A detached bow shock could form or the separation could extend to the origin of the boundary layer. Experimental values of mean pressures near the nose of the body indicate that the latter configuration may predominate for body thicknesses sufficiently large relative to the length of the plate upstream of the body, but no steady configurations of either type were observed.

The analysis developed for wedge-type dead-air regions was also applied to conical dead-air regions ahead of axially symmetric bodies, but for this case quantitative estimates must await theoretical or experimental determination of the skin friction on cones in the pressure of an initial boundary layer at supersonic speeds.

Lewis Flight Propulsion Laboratory,
National Advisory Committee for Aeronautics,
Cleveland, Ohio, May 2, 1951.

APPENDIX A

SYMBOLS

The following symbols are used in this report:

A	area
a	radius of rod ahead of axially symmetric blunt body
b	thickness of two-dimensional body or radius of axially symmetric body at point of contact with dead-air region
h	form factor, δ^*/θ
$k(M_0)$	function of M_0 which when multiplied by $R^{-1/\eta}$ yields friction drag coefficient
L	distance in x-direction from start of boundary layer to point of body where thickness or radius is b
l	distance from start of boundary layer to beginning of dead-air region
M	Mach number
N	power-law profile parameter for turbulent boundary layer, assumed equal to 7
P	pressure coefficient, $\dfrac{\frac{p}{p_0} - 1}{\frac{\gamma}{2} M_0^2}$
Pr	Prandtl number
p	static pressure
Q	function of M_0 and λ defined by equation (3)
Q_c	function of M_0 and λ_c defined by equation (12)
R	Reynolds number, based on distance given by subscripts
r	radius of nose of circular-nosed bodies
s	distance normal to cone or wedge surface
T	function of M_0 and λ defined by equation (6)
T_c	function of M_0 and λ_c defined by equation (14)

u	local velocity
x	distance in free-stream direction
y	distance normal to free-stream direction
γ	ratio of specific heats
δ	boundary-layer thickness
δ^*	displacement thickness of boundary layer
ϵ	factor of proportionality between change in θ on flat plate and along dead-air region
η	power parameter in skin-friction laws
φ	shock angle resulting from dead-air region
λ	angle of boundary of dead-air region
τ	shear stress
θ	momentum thickness of boundary layer
ρ	density
β	ratio of skin friction on cone to skin friction on wedge

Subscripts:

av	average
0	conditions ahead of dead-air region
1	conditions downstream of shock or at downstream end of dead-air region
c	conditions on surface of cone used to replace conical dead-air region
p	flat-plate value
la	laminar value
max	maximum
t	turbulent value

Primes denote differentiation with respect to x

APPENDIX B

LAMINAR BOUNDARY LAYER WITH TURBULENT SHEAR ON SEPARATION WEDGE

The general equation for evaluating the separation angle is (see equation (6)):

$$\epsilon \frac{\theta_0'}{\theta_0} b = T \tan \lambda \tag{B1}$$

It is desired to compare the values of b obtained for a given T and λ (or M_0 and λ) under two assumptions:

(1) Laminar flow on plate and on replacing wedge

(2) Laminar flow on plate and turbulent flow on replacing wedge

If values corresponding to assumptions (1) and (2) are identified with subscripts 1 and 2, respectively, the following relation applies for given M_0 and λ:

$$\left(\frac{\theta_0'}{\theta_0} b\right)_1 = \left(\frac{\theta_0'}{\theta_0} b\right)_2$$

or

$$\frac{b_2}{b_1} = \frac{(\theta_0'/\theta_0)_1}{(\theta_0'/\theta_0)_2} \tag{B2}$$

Now $(\theta_0'/\theta_0)_1 = \frac{1}{2l_1}$ from equation (8) of the text. In the quantity $(\theta_0'/\theta_0)_2$, θ_0 is the momentum thickness corresponding to a laminar run of distance l_2, whereas θ_0' is the turbulent friction coefficient corresponding to the momentum thickness θ_0. Thus,

$$\theta_{0_1} \equiv \theta_{0_2} = 2l_2 k_{la} R_{l_2}^{-1/2} = \frac{7}{6} l_2' k_t R_{l_2}'^{-1/7} = \frac{7}{6} l_2' \theta_{0_2}'$$

where l_2' is the equivalent turbulent run required to build up the actual momentum thickness θ_0. From these equations,

$$\left(\frac{\theta_0'}{\theta_0}\right)_2 = \frac{6}{7l_2'}$$

and

$$\frac{l_2'}{l_2} = \frac{12}{7}\frac{k_{la}R_{l_2}^{-1/2}}{k_t R_{l_1}^{-1/7}} = \frac{12}{7}\frac{k_{la}}{k_t}\frac{R_{l_2}^{-1/2}}{R_{l_2}^{-1/7}\left(\frac{l_2'}{l_2}\right)^{-1/7}}$$

or

$$l_2' = l_2\left(\frac{12}{7}\frac{k_{la}}{k_t}R_{l_2}^{-5/14}\right)^{7/6}$$

Equation (B2) now becomes

$$\frac{b_2/l_2}{b_1/l_1} = \left(\frac{12}{7}\right)^{1/6}\left(\frac{k_{la}}{k_t}R_{l_2}^{-5/14}\right)^{7/6} = 1.094\left(\frac{k_{la}}{k_t}R_{l_2}^{-5/14}\right)^{7/6} \quad \text{(B3)}$$

To estimate the magnitude of the difference resulting from cases (1) and (2), assume that k_{la}/k_t is nearly independent of Mach number and has the incompressible value[4]

$$\frac{k_{la}}{k_t} = \frac{1.328}{0.0131} = 101.3 \approx 100$$

Then

$$\frac{b_2/l_2}{b_1/l_1} = \frac{235}{R_{l_2}^{0.416}} \quad \text{(B4)}$$

---

[4]The value of k_{la}/k_t obtained for $M_0 = 1.9$ from equations in references 1 and 2 is 103.2 for the Reynolds number of the tests reported herein.

If the models are placed at the distance L from the leading edge of the plate, equation (B4) becomes

$$\frac{b_2/L}{\left[1 - \frac{b_2}{L} \operatorname{ctn} \lambda\right]^{0.584}} = \frac{235}{R_L^{0.416}} \frac{b_1/L}{1 - \frac{b_1}{L} \operatorname{ctn} \lambda} \tag{B5}$$

From equation (B5), b_2/L can be calculated from b_1/L for any value of M_0 and λ. As might be expected, the variation of b_2/L with λ or φ is no longer independent of Reynolds number. Values of b/L obtained from equation (B5) for two values of L are compared with the purely laminar values in figure 9.

APPENDIX C

COMPUTATION OF SEPARATION ANGLE WHEN UPSTREAM BOUNDARY LAYER IS PARTLY LAMINAR

The extent of the laminar region before transition influences the separation angle through the magnitude of θ_0, which is proportional to the integrated friction drag up to the separation point. The separation angle can be calculated as function of b/L for this case if the transition is assumed to occur at a definite point, $x = l_1$, and if the value of θ at this point can be estimated. For the present purpose, it is assumed that the jump in θ at l_1 is one-half the difference between the value of θ obtained with the turbulent equation and the value of θ obtained with the laminar equation. This assumption represents a compromise between two conventional assumptions, namely, that there is no discontinuity in θ at a transition point or that the jump in θ at the transition point is such that the values of θ beyond the transition point are the same as they would be with turbulent flow from the leading edge. The relative magnitudes of θ_0 resulting from these two assumptions are indicated in the following sketch. The compromise values used should be adequate for estimating the magnitude of the effect of a partly laminar boundary layer.

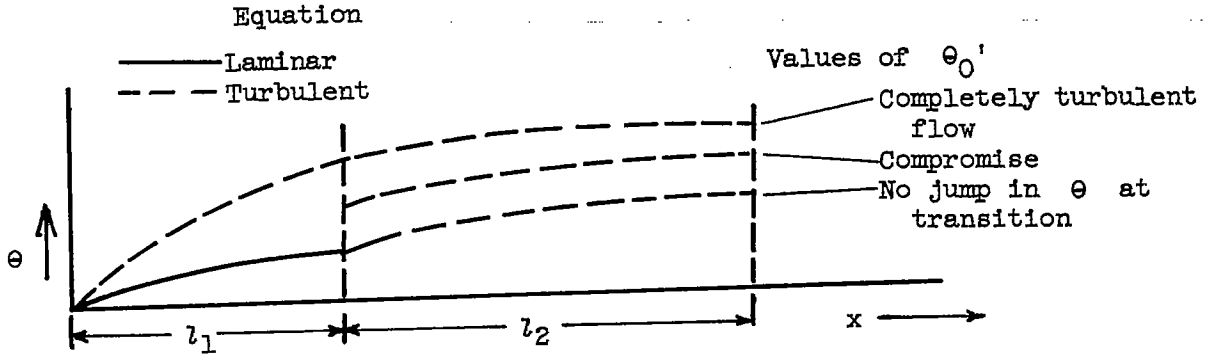

With this assumption the equation for θ_0 can be written:

$$\theta_0 = \int_0^{l_1} k_{la} R_x^{-1/2}\, dx + \frac{1}{2} l_1 \left(k_t R_{l_1}^{-1/7} - k_{la} R_{l_1}^{-1/2} \right) + \int_{l_1}^{l_2} k_t R_x^{-1/7}\, dx$$

$$= l_1 \left(\frac{3}{2} k_{la} R_{l_1}^{-1/2} - \frac{2}{3} k_t R_{l_1}^{1/7} \right) + \frac{7}{6} l_2 k_t R_{l_2}^{-1/7}$$

Since

$$\theta_0' = k_t R_{l_2}^{-1/7}$$

equation (6) in the text becomes

$$\epsilon \frac{\theta_0' b}{\theta_0} = T \tan \lambda = \frac{\epsilon b \, k_t R_{l_2}^{-1/7}}{l_1 \left(\frac{3}{2} k_{la} R_{l_1}^{-1/2} - \frac{2}{3} k_t R_{l_1}^{-1/7} \right) + \frac{7}{6} l_2 k_t R_{l_2}^{-1/7}} \tag{C1}$$

To compare the values of b obtained from equation (C1) with those obtained for completely turbulent flow, let $T \tan \lambda$ (or M_0 and λ) remain the same for both cases. If values corresponding to completely turbulent flow are denoted by the subscript α and those for partly laminar flow by subscript β,

$$\left(\frac{\theta_0' b}{\theta_0} \right)_\beta = \left(\frac{\theta_0' b}{\theta_0} \right)_\alpha = \frac{6}{7} \frac{b_\alpha}{l_2} \tag{C2}$$

After some algebraic manipulation, equations (C1) and (C2) result in the following equation:

$$\frac{(b/l_2)_\beta}{\left(\frac{l_1}{l_2} \right)^{6/7} \left(150 \, R_{l_1}^{-5/14} - \frac{2}{3} \right) + \frac{7}{6}} = \frac{6}{7} \left(\frac{b}{l_2} \right)_\alpha \tag{C3}$$

where k_{la}/k_t has been taken equal to 100, as in appendix B. Because $l_2 = L - b \operatorname{ctn} \lambda$, equation (3) can also be written

$$\frac{(b/L)_\beta \left[1 - \left(\frac{b}{L} \right)_\beta \operatorname{ctn} \lambda \right]^{1/7}}{\frac{6}{7} \left(\frac{l_1}{L} \right)^{6/7} \left(150 \, R_{l_1}^{-5/14} - \frac{2}{3} \right) + \left[1 - \left(\frac{b}{L} \right)_\beta \operatorname{ctn} \lambda \right]^{6/7}} = \frac{(b/L)_\alpha}{1 - \left(\frac{b}{L} \right)_\alpha \operatorname{ctn} \lambda} \tag{C4}$$

This equation can be solved for $(b/L)_\beta$ by trial when l_1 and the Reynolds number are known since $(b/L)_\alpha$ as a function of λ is known from computations for the case of completely turbulent boundary layers.

In figure 9, the variation of b/L with φ from equation (C4) for a 3/4-inch laminar run before transition is compared with the variation for completely turbulent flow and with experimental results.

REFERENCES

1. Tucker, Maurice: Approximate Calculation of Turbulent Boundary-Layer Development in Compressible Flow. NACA TN 2337, 1951.

2. Chapman, Dean R., and Rubesin, Morris W.: Temperature and Velocity Profiles in the Compressible Laminar Boundary Layer with Arbitrary Distribution of Surface Temperature. Jour. Aero. Sci., vol. 16, no. 9, Sept. 1949, pp. 547-565.

3. Moeckel, W. E.: Approximate Method for Predicting Form and Location of Detached Shock Waves Ahead of Plane or Axially Symmetric Bodies. NACA TN 1921, 1949.

4. Pearce, R. B.: Shock Waves on Surfaces with Thick Boundary Layers. Rep. No. AL-399, North American Aviation, Inc. (Los Angeles), Dec. 30, 1947.

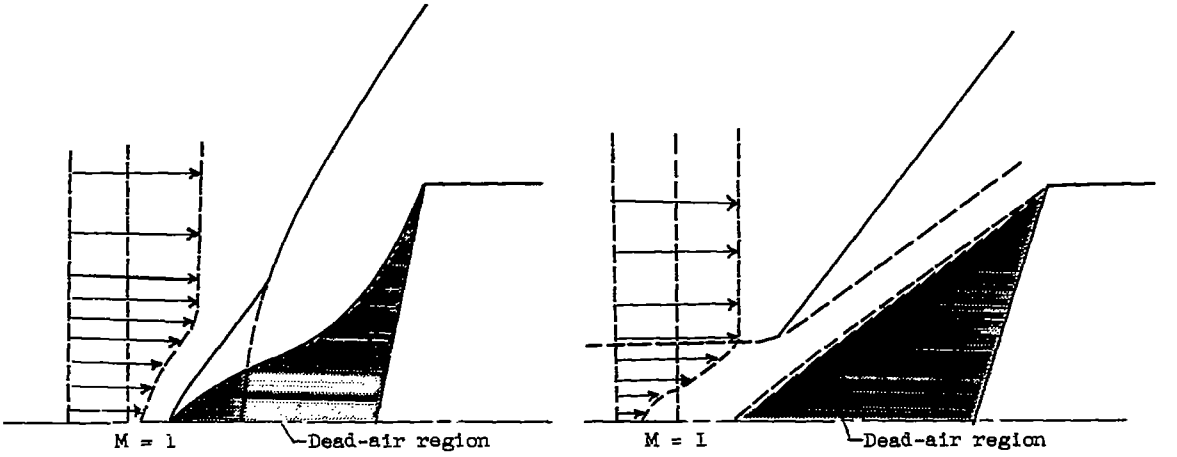

(a) Supersonic initial velocities. (b) Partly subsonic initial velocity.

Figure 1. - Flow against blunt bodies in nonuniform stagnation pressure field.

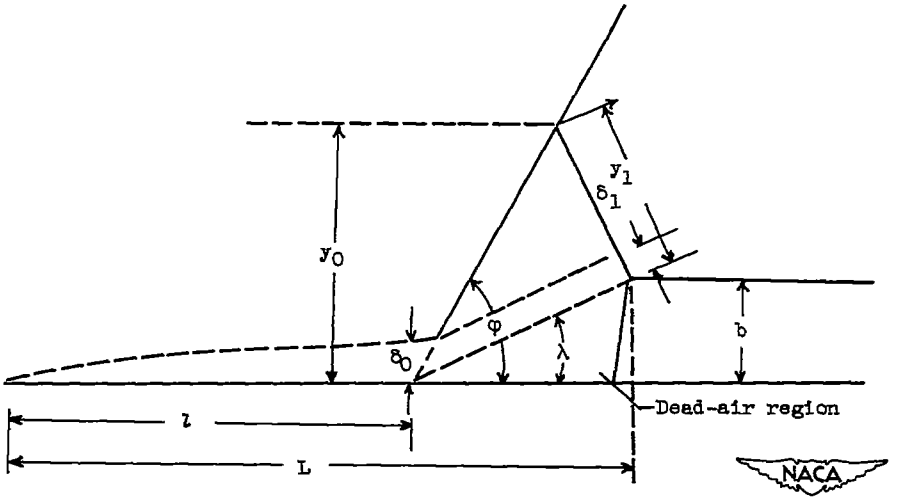

Figure 2. - Sketch used for analysis of flow against blunt bodies mounted on flat plate.

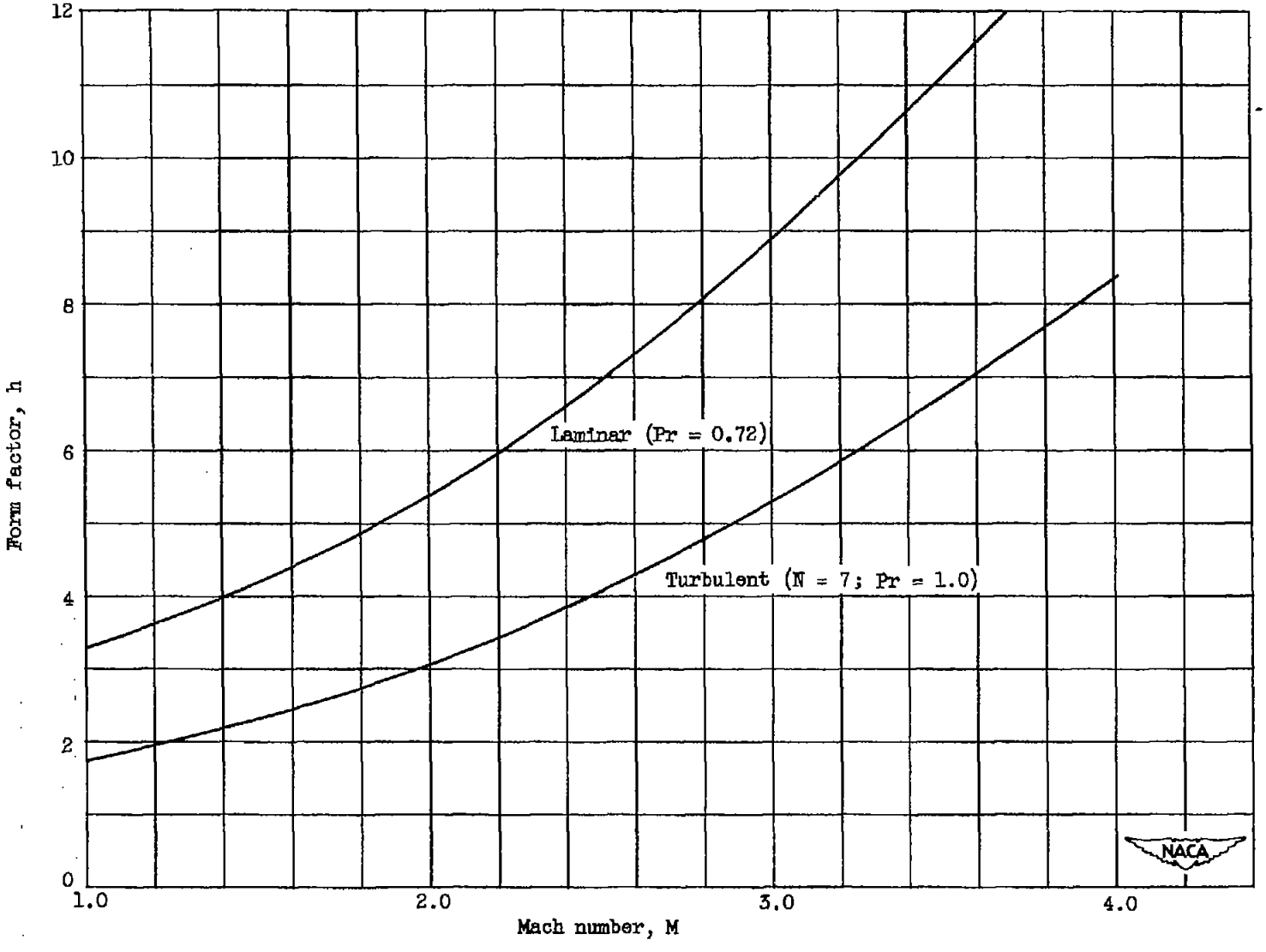

Figure 3. - Form factor for laminar and turbulent compressible, flat-plate boundary-layer profiles as function of free-stream Mach number.

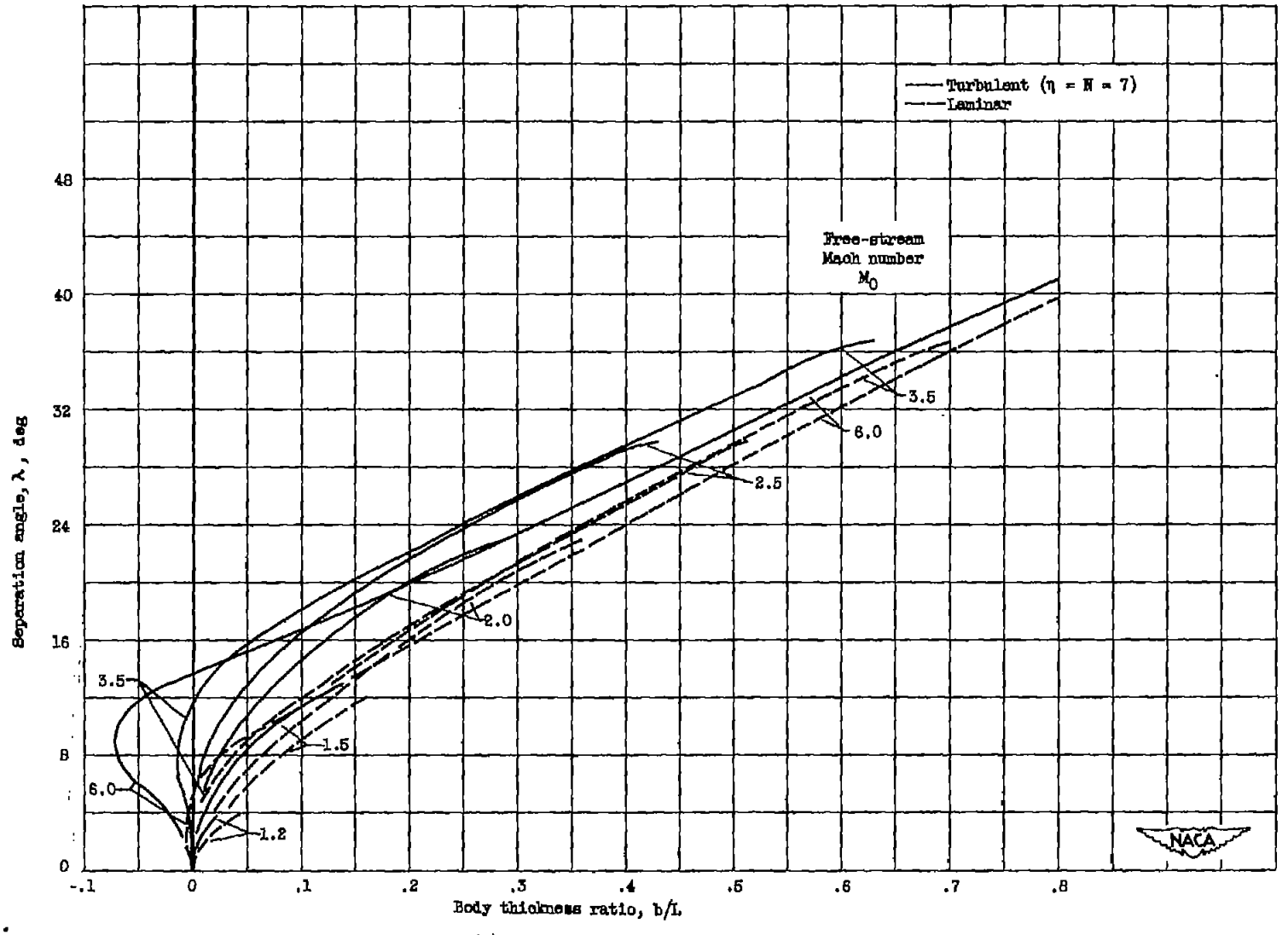

(a) Separation angle.

Figure 4. - Variation of separation angle and shock angle with body thickness ratio. Two-dimensional flow.

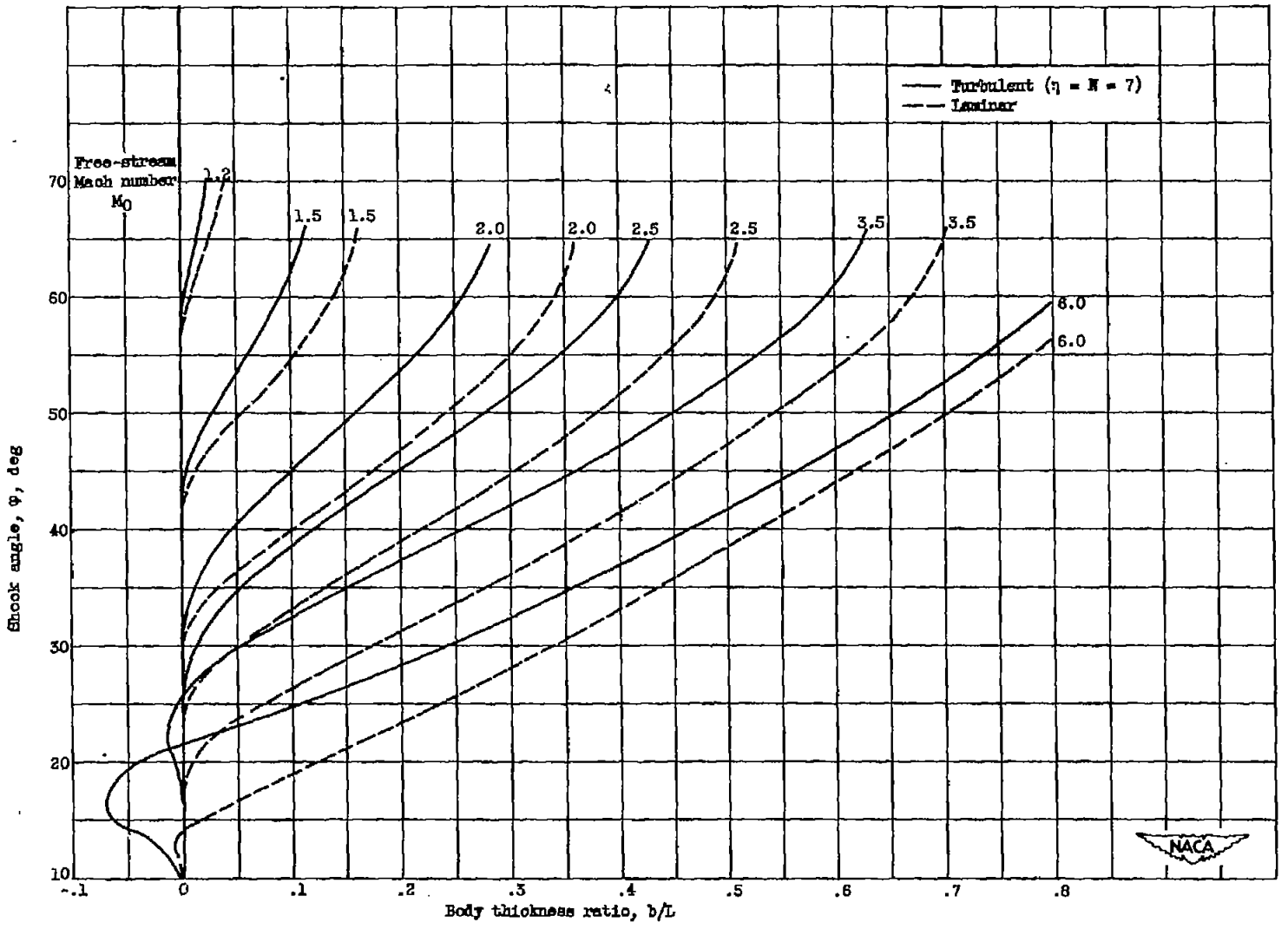

(b) Shock angle.

Figure 4. - Concluded. Variation of separation angle and shock angle with body thickness ratio. Two-dimensional flow.

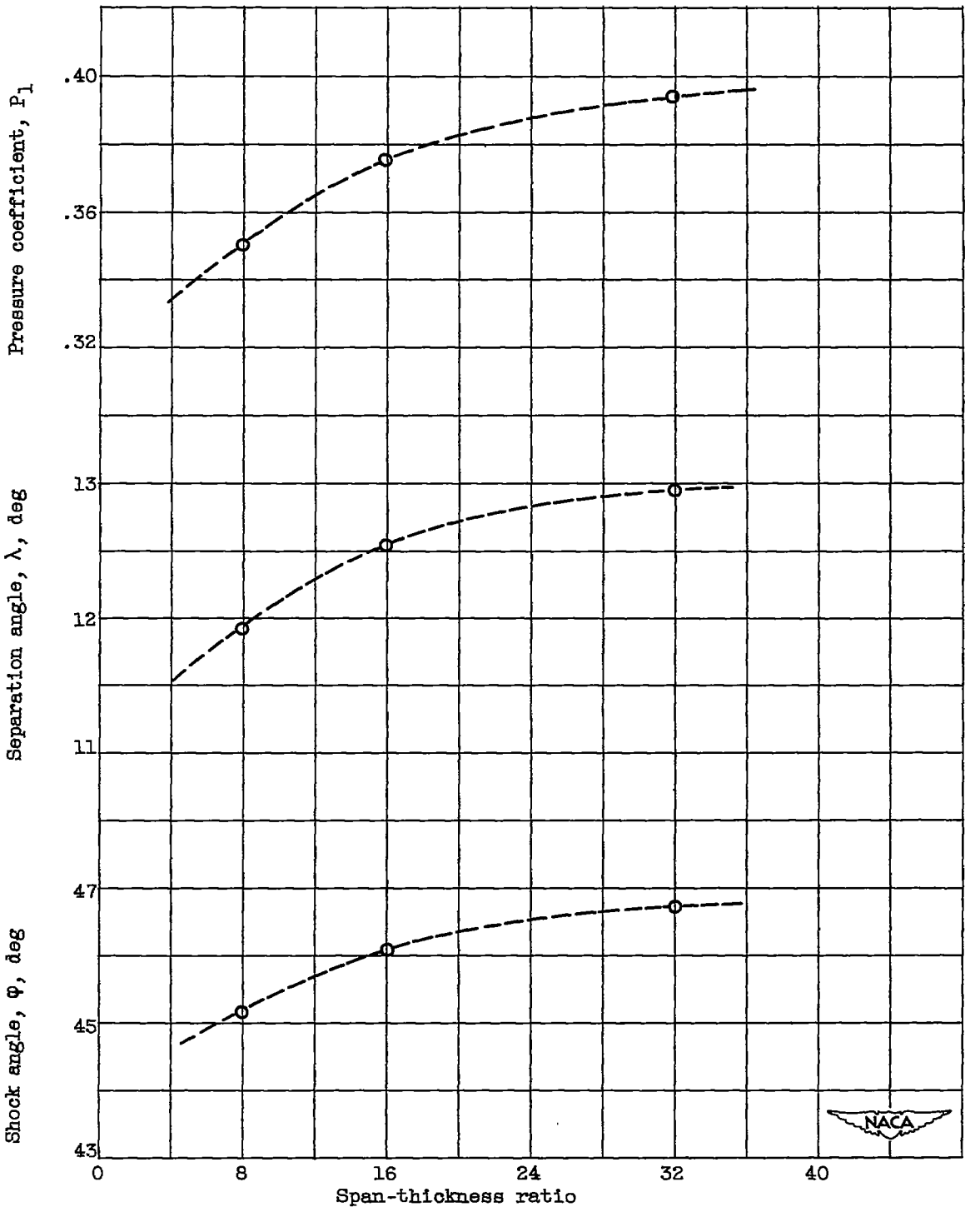

Figure 5. - Effect of span-thickness ratio on separation parameters. Free-stream Mach number M_0, 1.84; b, 0.5 inch; L, 5.25 inches.

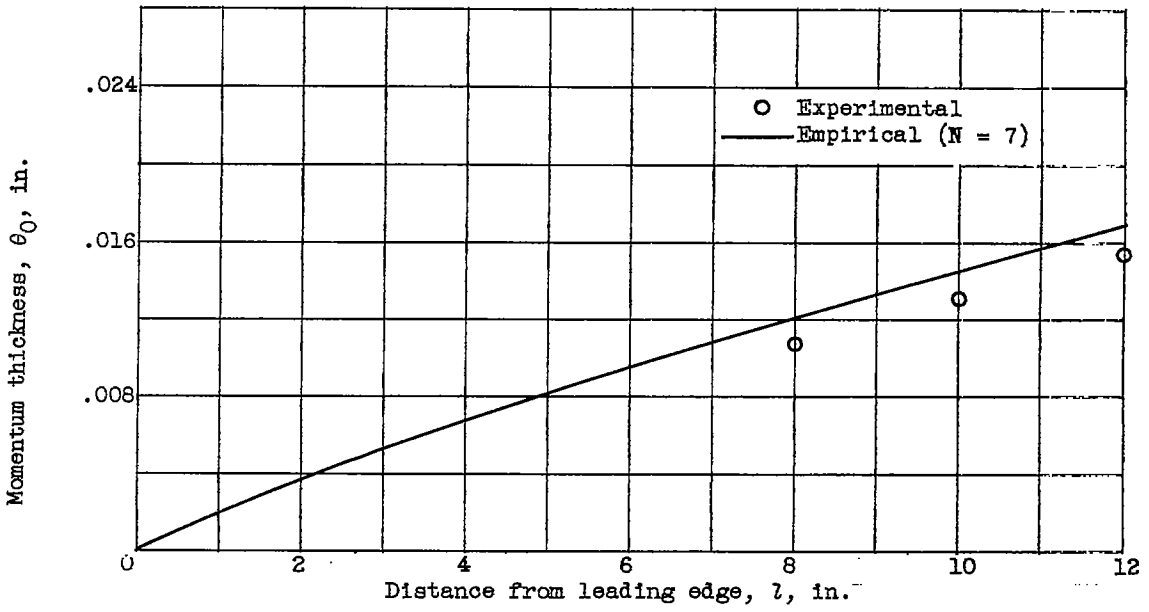

(a) Momentum thickness, θ_0.

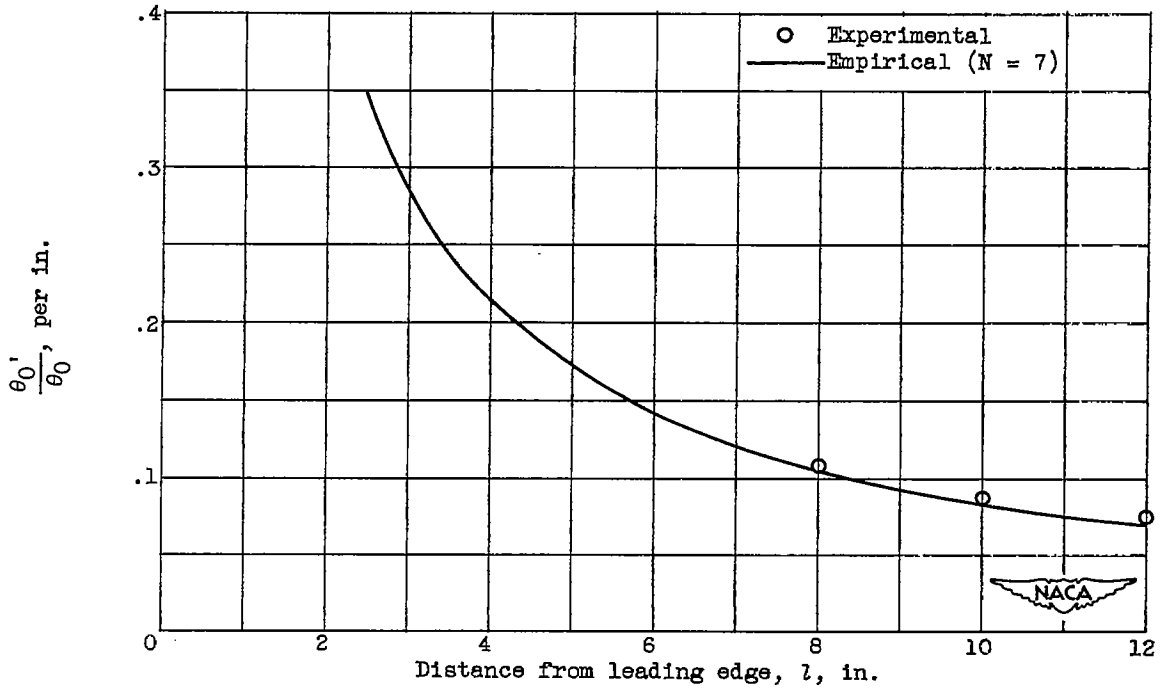

(b) Ratio of θ_0' to θ_0.

Figure 6. - Experimental and empirical boundary-layer parameters for flat plate used in tests. Artificial transition; free-stream Mach number M_0, 1.88.

(a) Free-stream Mach number M_0, 1.84; b, $\frac{1}{4}$ inch; L, $8\frac{1}{2}$ inches; artificial transition.

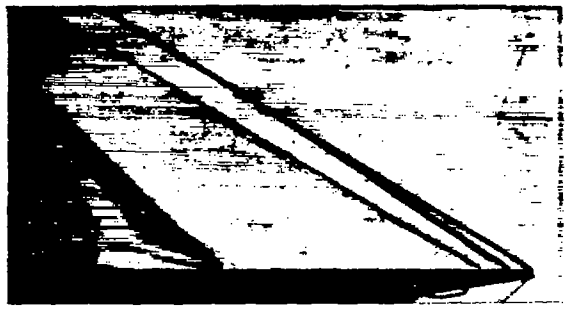

(b) Free-stream Mach number M_0, 1.84; b, $\frac{1}{2}$ inch; L, $8\frac{1}{2}$ inches; artificial transition.

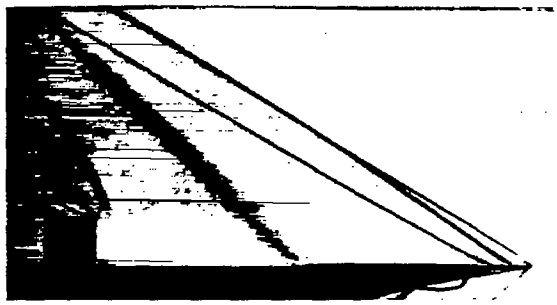

(c) Free-stream Mach number M_0, 1.84; b, 1 inch; L, $8\frac{1}{2}$ inches; artificial transition.

(d) Free-stream Mach number M_0, 1.84; b, $1\frac{9}{16}$ inches; L, $8\frac{1}{2}$ inches; artificial transition.

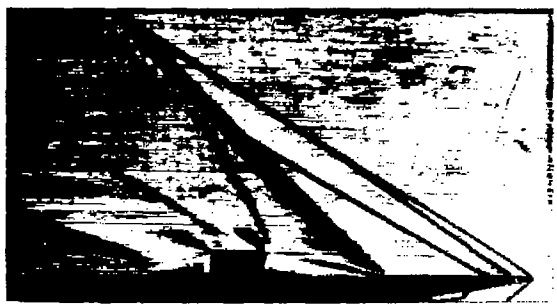

(e) Free-stream Mach number M_0, 1.84; b, $\frac{1}{2}$ inch; L, $5\frac{1}{4}$ inches; artificial transition.

(f) Free-stream Mach number M_0, 1.87; b, $\frac{3}{4}$ inch; L, $8\frac{1}{2}$ inches; natural transition.

NACA
C-27618

Figure 7. - Schlieren photographs of flow against rectangular rods mounted on flat plate.

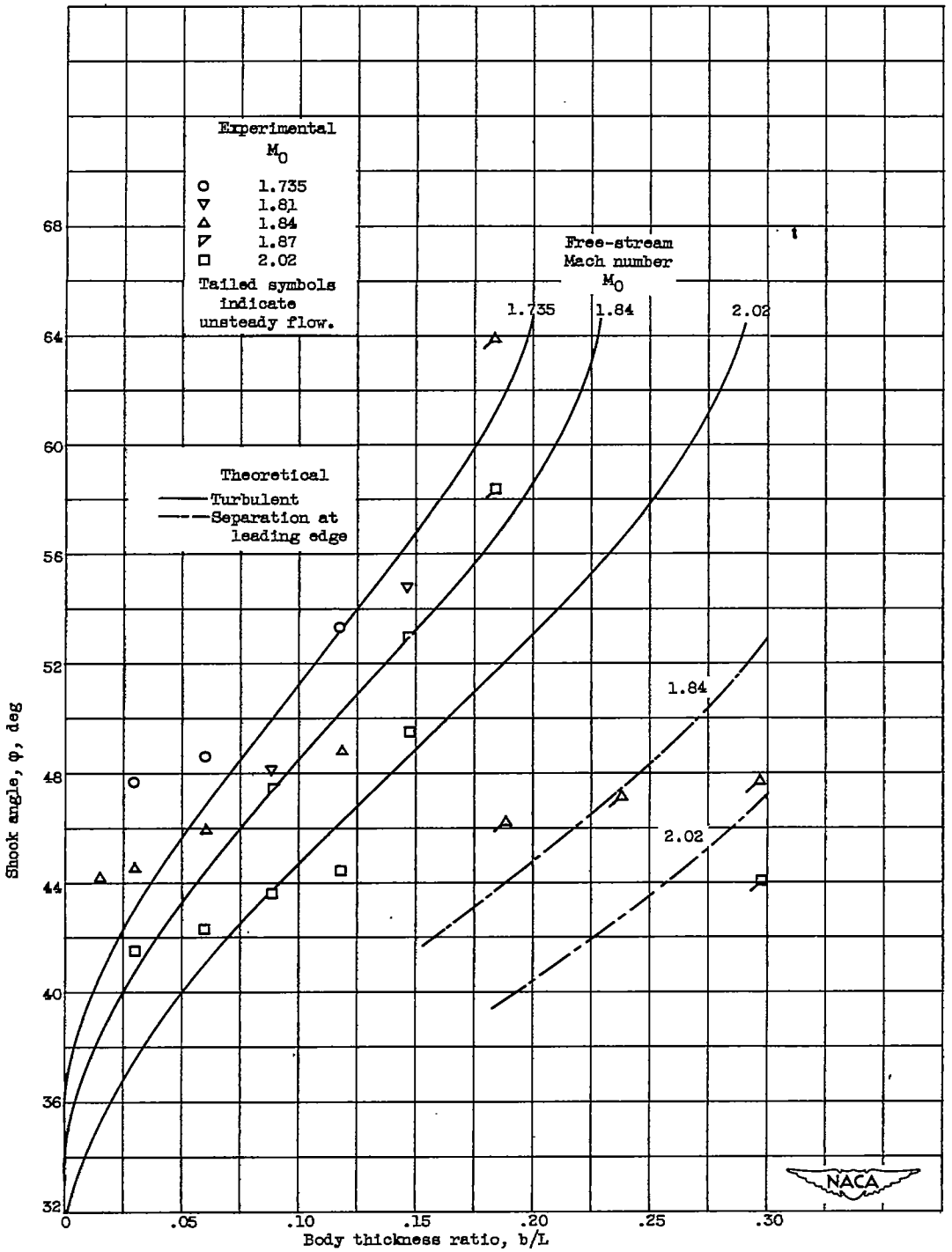

(a) Uncorrected data.

Figure 8. - Comparison of experimental and theoretical variation of separation shock angle with body thickness ratio. L, $8\frac{1}{2}$ inches; artificial transition.

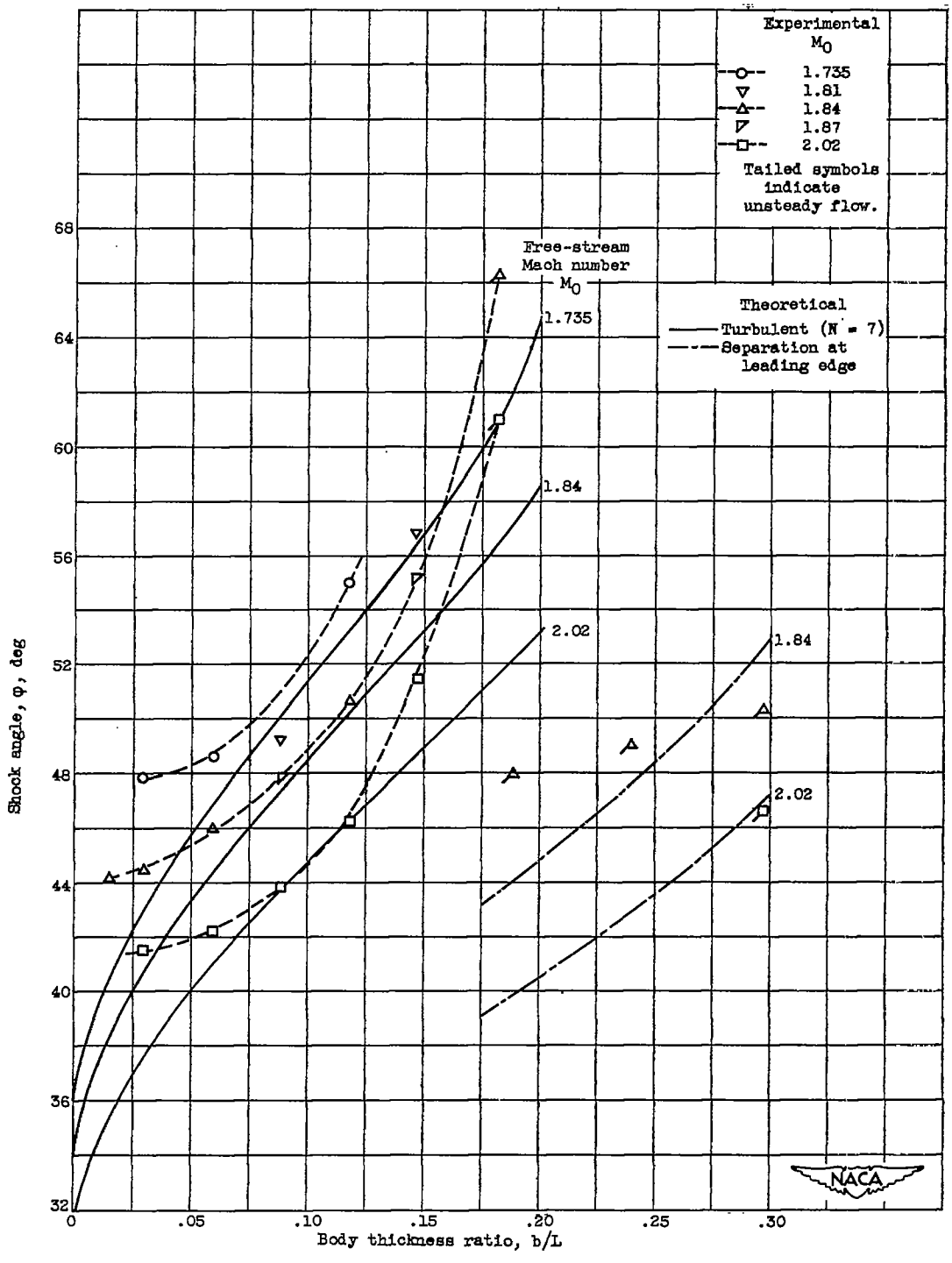

(b) Corrected data.

Figure 8. - Continued. Comparison of experimental and theoretical variation of separation shock angle with body thickness ratio. L, $8\frac{1}{2}$ inches; artificial transition.

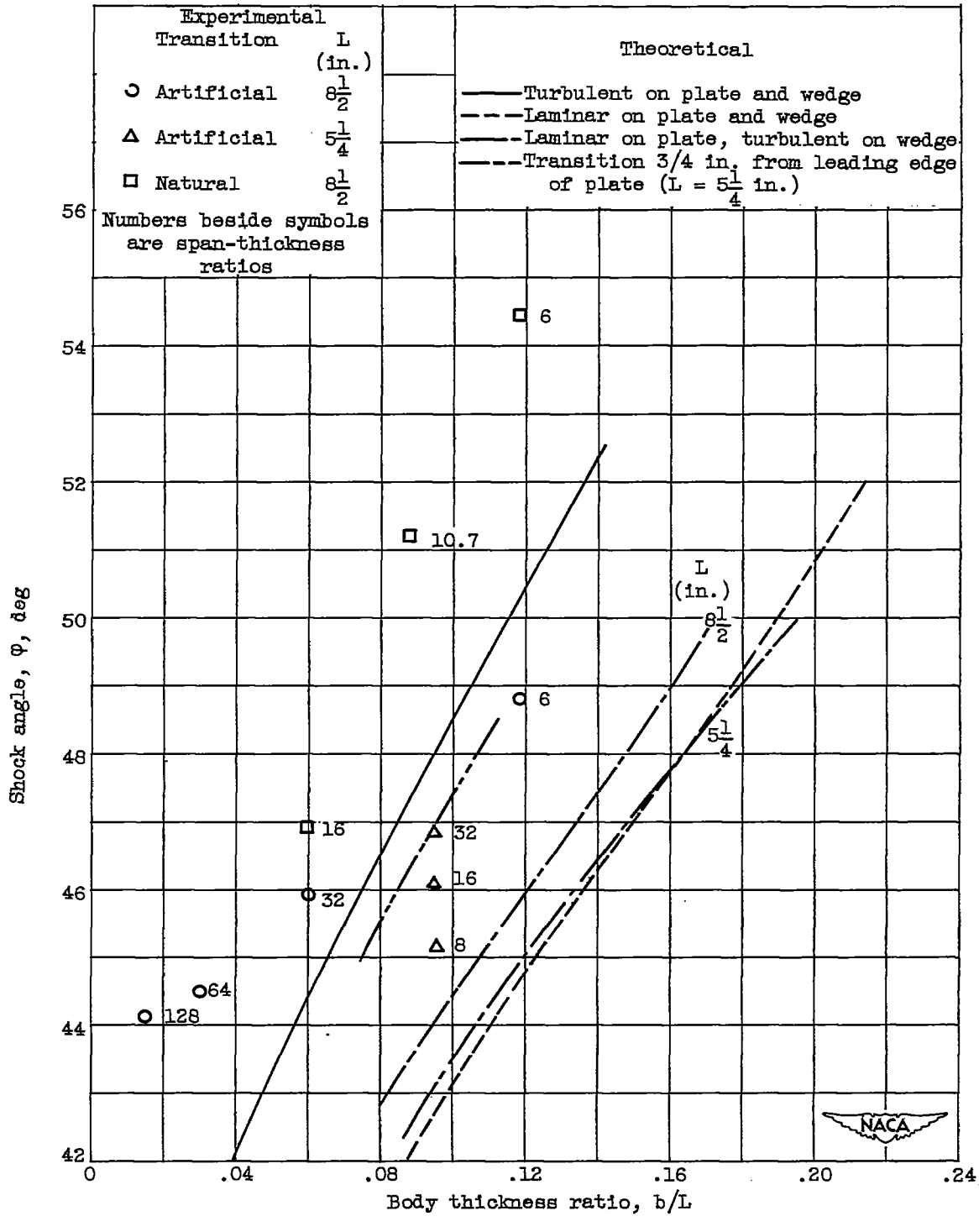

Figure 9. - Effect of changes in boundary layer ahead of separation point. Free-stream Mach number M_0, 1.84.

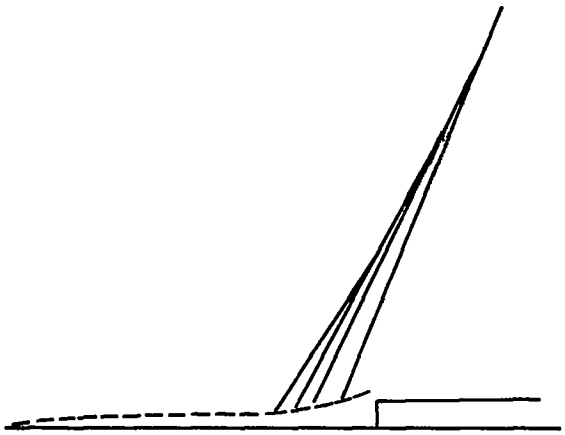

(a) $0<b/L<0.05$.

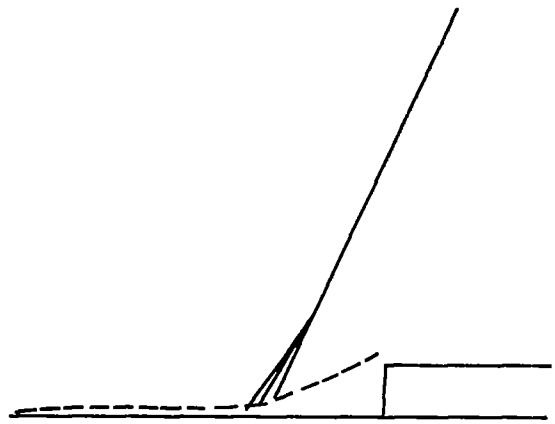

(b) $0.05<b/L<0.13$.

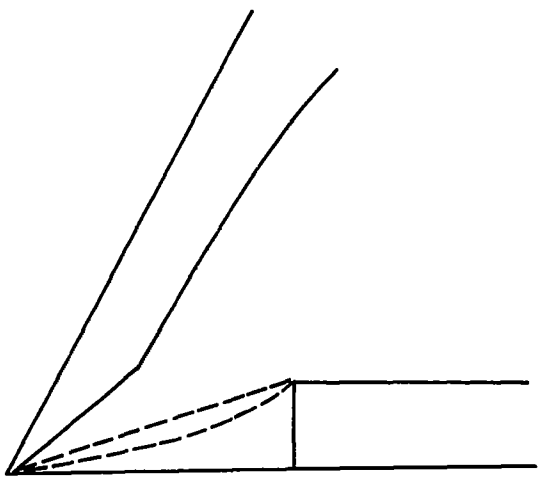

(c) $0.13<b/L<\tan^{-1}\lambda_{max}$ (unsteady flow).

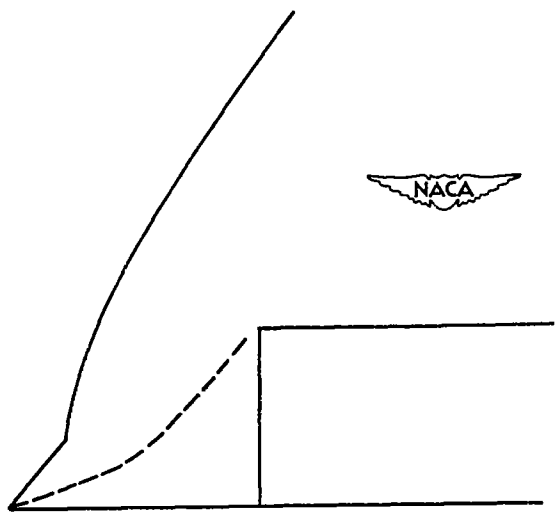

(d) $\tan^{-1}\lambda_{max}<b/L<\infty$.

Figure 10. - Observed and probable flow regimes for various ranges of body thickness ratio. Free-stream Mach number M_0, approximately 1.9.

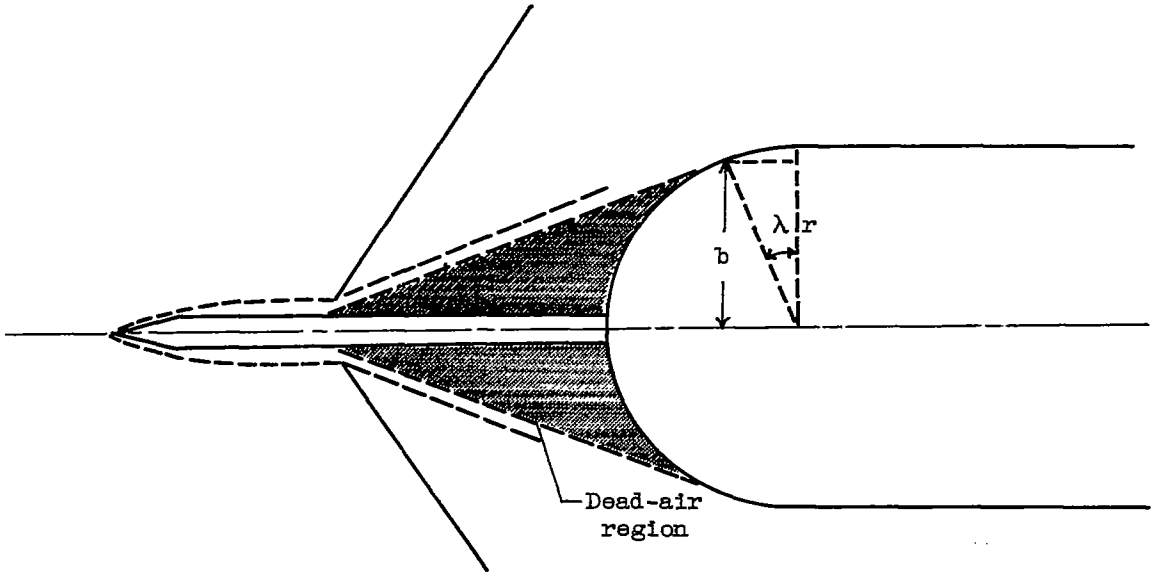

Figure 11. - Reduction of drag of thick bodies by provision of initial boundary layer.

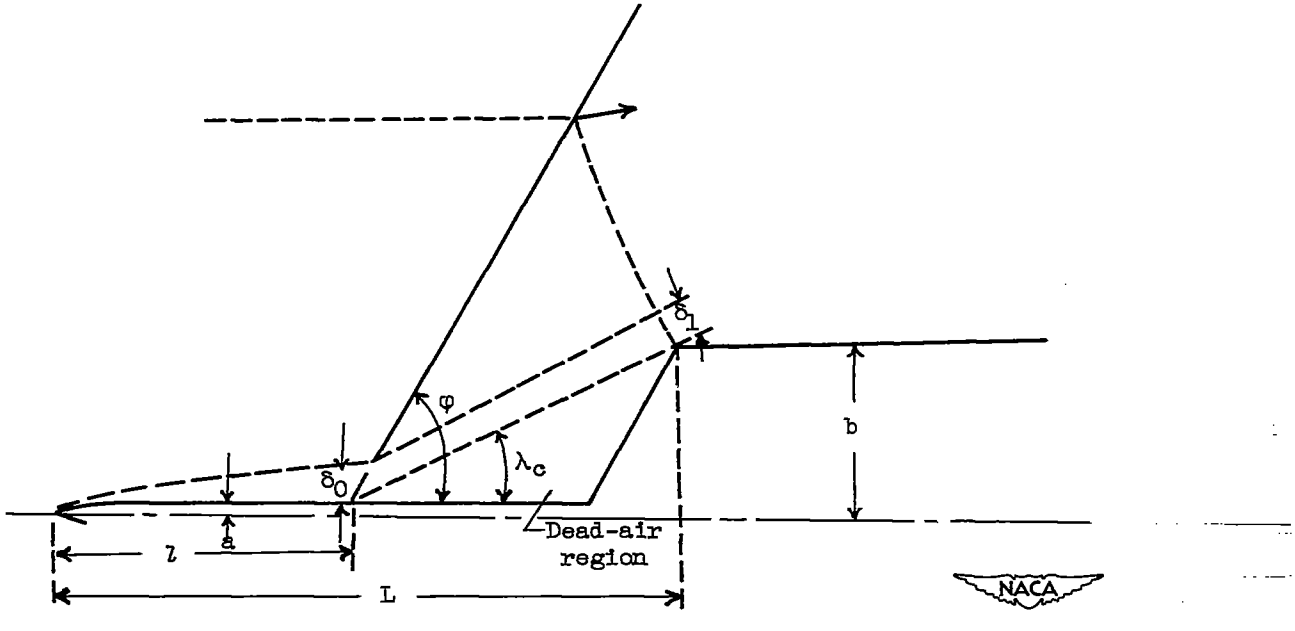

Figure 12. - Sketch for analysis of axially symmetric flow against blunt bodies with initial boundary layer.